Synergistic tumor growth-inhibitory effect of the prostate-specific antigen-activated fusion peptide BSD352 for prostate cancer therapy

Bin Li, Li-Jun Zhang, Zhou-Liang Zhang, Min Long, Ji-Hong Ren, Fang Lin, Xi Wang, Jun-Xia Wei, Ke Dong and Hui-Zhong Zhang

Prostate-specific antigen (PSA), a serine protease, is a promising target for the development of prodrugs in prostate cancer treatment. In this study, we designed a novel fusion peptide, BSD352, containing three functional domains: a protein transduction domain from HIV transactivating regulatory protein (TAT) followed by the BH3 domain of the p53 upregulated modulator of apoptosis (TAT-BH3), an anti-vascular endothelial growth factor peptide (SP5.2), and an anti-basic fibroblast growth factor peptide (DG2). These different domains in BSD352 were linked together by a linker sequence corresponding to a PSA hydrolytic substrate peptide. The BSD352 fusion peptide could be selectively cleaved by PSA in PSA-producing LNCaP prostate cancer cells. Furthermore, the BSD352 fusion peptide was efficiently transduced into tumor cells both *in vitro* and *in vivo*, and the BH3 domain was found to induce tumor cell apoptosis by elevating the expression of Bax, cytochrome C release, and caspase-9 cleavage. Moreover, the SP5.2 and DG2 domains in the BSD352 fusion peptide also exhibited in-vitro endothelial cell growth inhibition and in-vivo antiangiogenic activities. Direct injection of BSD352 into an established LNCaP xenograft tumor in mice inhibited tumor growth, whereas a synergistic effect was observed with the combined use of wild-type BH3, SP5.2, and DG2 functional domains. These results suggest that BSD352 could be beneficial for the treatment of accessible prostate tumors and may provide a complementary strategy for prostate cancer therapy. *Anti-Cancer Drugs* 22:213–222 © 2011 Wolters Kluwer Health | Lippincott Williams & Wilkins.

Anti-Cancer Drugs 2011, **22**:213–222

Keywords: antiangiogenesis, BH3, fusion peptide, prostate cancer, prostate-specific antigen

Department of Laboratory Medicine, Tangdu Hospital, Fourth Military Medical University, Xi'an, China

Correspondence to Hui-Zhong Zhang, Department of Laboratory Medicine, Tangdu Hospital, Fourth Military Medical University, Xinsi Road 710038, Xi'an, China
Tel: +86 29 84777470; fax: +86 29 84777654;
e-mail: zhz328@yahoo.com.cn

Bin Li and Li-Jun Zhang contributed equally to this study and should be regarded as joint first authors

Received 30 June 2010 **Revised form accepted** 2 September 2010

Introduction

Prostate carcinoma is the second leading cause of cancer death in males [1,2]. Clinically, most localized prostate cancers are androgen dependent and can be treated by surgical resection or radiation therapy [3–5]. However, advanced prostate cancers, either at invasive or even micrometastatic stages, present a clinical challenge as these tumors respond poorly to standard cytotoxic regimens. Therefore, prostate cancers are treated based on their unique characteristics, in that they are exquisitely dependent on androgen for growth and survival [6–8]. As androgen ablation triggers the cell death or cell cycle arrest of prostate cancer cells [9–11], it remains the primary course of treatment for all patients with metastatic disease [12,13]. Unfortunately, despite the efficacy of androgen ablation at an early stage, many advanced-stage prostate cancers relapse into an androgen-independent form that results in high mortality rates.

The development of new therapeutic strategies for the treatment of hormone refractory prostate cancer is imperative, and there is a great interest in identifying alternative approaches that can improve efficacy and reduce the side effects of the treatment [14,15]. Prostate cancer cells produce high levels of prostate-specific antigen (PSA), which is enzymatically active in the extracellular fluid surrounding prostate cancers, but is found at a 1000-fold to 10 000-fold lower concentration in the circulating fluid where it is also inactivated because of binding to abundant serum protease inhibitors. The exclusive presence of high levels of active PSA within the prostate cancer sites makes PSA an attractive target for the development of new therapeutics [16].

Currently, promising strategies for the treatment of malignant tumor are being investigated from three aspects: development of drugs that induce cancer cell apoptosis by different mechanisms, interruption of proangiogenic stimuli, and the inhibition of growth factor receptor-dependent signaling pathways. Of particular interest, the mitochondrial apoptotic pathway is, to a large extent, regulated by Bcl-2 family proteins. It has been shown that the p53 upregulated modulator of apoptosis BH3 domain can effectively induce cell apoptosis by

0959-4973 © 2011 Wolters Kluwer Health | Lippincott Williams & Wilkins DOI: 10.1097/CAD.0b013e3283401f4d

binding to the antiapoptotic Bcl-2 family proteins, activating the effector protein of Bax, and triggering the release of cytochrome C from the mitochondria. On the other hand, angiogenesis has been shown to correlate with tumor progression, higher recurrence risk, and poor prognosis. Notably, the vascular endothelial growth factor (VEGF) and the basic fibroblast growth factor (bFGF) are two of the most important proangiogenic stimuli and are overexpressed in most malignant tumor cells [17–19].

The protein transduction domains (PTDs) are short stretches of positively charged amino acids that enable the proteins that contain them to enter the cells efficiently. In particular, the 11-amino-acid region of the HIV transactivating regulatory protein (TAT) PTD, when fused to even large proteins, has been shown to increase the ability of the protein to cross cell membranes dramatically [20,21].

In this study, we designed a novel fusion peptide BSD352 that is composed of three functional domains, a TAT followed by the BH3 domain, an anti-VEGF peptide (SP5.2) [22], and an anti-bFGF peptide (DG2) [23], which are linked by two PSA hydrolytic substrate (PHS) peptides. Our results show that the BSD352 fusion peptide induces tumor cell apoptosis *in vitro* and exhibits tumor growth inhibition activity *in vivo* on PSA-producing prostate cancer cells.

Materials and methods

Design of oligonucleotides and construction of fusion peptides expression vectors

The following peptides were designed: (i) BSD352 that contains three functional peptides including TAT-BH3, SP5.2, and DG2. (ii) B_mSD352 in which the BH3 peptide was mutated, (iii) BS_mD_m352 in which both the SP5.2 and DG2 peptides were mutated (iv) $B_mS_mD_m352$ in which all the three functional peptides were mutated, and (v) BGSD352 in which a full-length enhanced green fluorescent protein from a pGL3-basic vector, as described earlier in our laboratory [24], was inserted downstream of the BH3 peptide in the sequence shown in Fig. 1a. The oligonucleotides corresponding to the different functional peptides and the PHS peptide were back-translated from the amino acid sequence using the codons optimized for *Escherichia coli* expression, and the restriction enzyme sites that were incorporated to facilitate ligation are italicized (Table 1). To express the fusion peptides, the full-length cDNA of BSD352, B_mSD352, BS_mD_m352, and $B_mS_mD_m352$ were chemically synthesized (Augct Biotechnology Inc., Beijing, China). A His-tag segment was fused to the C-terminus of all the fusion peptides for single-step purification. The coding sequences for different fusion proteins were confirmed by sequencing and then cloned into the pET-32a (+) (Novagen, Madison, Wisconsin, USA) vector for protein expression and purification.

Expression and purification of fusion proteins

E. coli strain BL21 (DE3) codon + was grown overnight at 37°C in Luria–Bertani broth supplemented with 100 mg/ml ampicillin, and protein expression was induced by the addition of 1 mmol/l isopropyl-β-D-thiogalactoside (Gibco, Grand Island, New York, USA). Bacteria were collected and purification was carried out through a nickel-nitriloacetic acid column (Amersham Bioscience, Sweden) according to the manufacturer's protocol. Purified fusion proteins were filtered through a 0.2 μmol/l membrane, and were then analyzed by western blot analysis using the anti-His antibody. Protein concentrations were determined by the Bradford test (Bio-Rad, California, USA).

Cell culture

Prostate cancer cell lines, LNCaP (PSA-producing) cells, PC3 (non-PSA producing) cells, and RWPE-1 cells (human prostatic epithelial cells, supplied by Xiao-Jian Yang, Xijing Hospital of the Fourth Military Medical University) were grown in RPMI 1640 medium (Gibco) containing 10% fetal bovine serum (Gibco) plus 1% penicillin–streptomycin and 1% L-glutamine. HUVE cells were isolated from umbilical cords by collagenase treatment and cultured in M199 medium (Gibco) supplemented with 20% fetal bovine serum. All cells were maintained at 37°C in a humidified 5% CO_2 containing incubator.

Intracellular translocation of fusion peptides

LNCaP, PC3, and RWPE-1 cells seeded in six-well plates or on coverslips in a 24-well plate were incubated with the BGSD352 fusion protein at a concentration of 45 μmol/l for 4 h. The cells in the six-well plates were harvested by trypsin treatment and the presence of the BGSD fusion protein (containing a His-tag) in the tumor cells was detected by western blot analysis with the anti-His antibody. The cells grown on coverslips were fixed in methanol/acetone (1 : 1) and then incubated with a solution of SlowFade (Molecular Probe, Carlsbad, California, USA). The green fluorescence of the enhanced green fluorescent protein was observed under a fluorescence microscope (Olympus, Tokyo, Japan).

Cell growth inhibition assay

LNCaP, PC3, RWPE-1, and HUVE cells were placed in 96-well plates (Costar, Milpitas, California, USA) at 3×10^4 in 200 μl of complete RPMI 1640 medium overnight. For TAT-BH3 function, the LNCaP, PC3, and RWPE-1 cells were incubated with BS_mD_m352 and $B_mS_mD_m352$ at a concentration ranging from 5 to 90 μmol/l for 4 to 24 h. To study the antiangiogenesis effect, the HUVE cells were incubated with PSA (Merck Biosciences, USA) predigested B_mSD352 and $B_mS_mD_m352$ at concentrations ranging from 5 to 90 μmol/l for 4 to 24 h. The cell proliferation was detected using the MTT Cell Proliferation and Cytotoxicity Assay Kit (Beyotime Biotechnology, China) according to the manufacturer's instructions. Absorbance (*A*) was measured at

Fig. 1

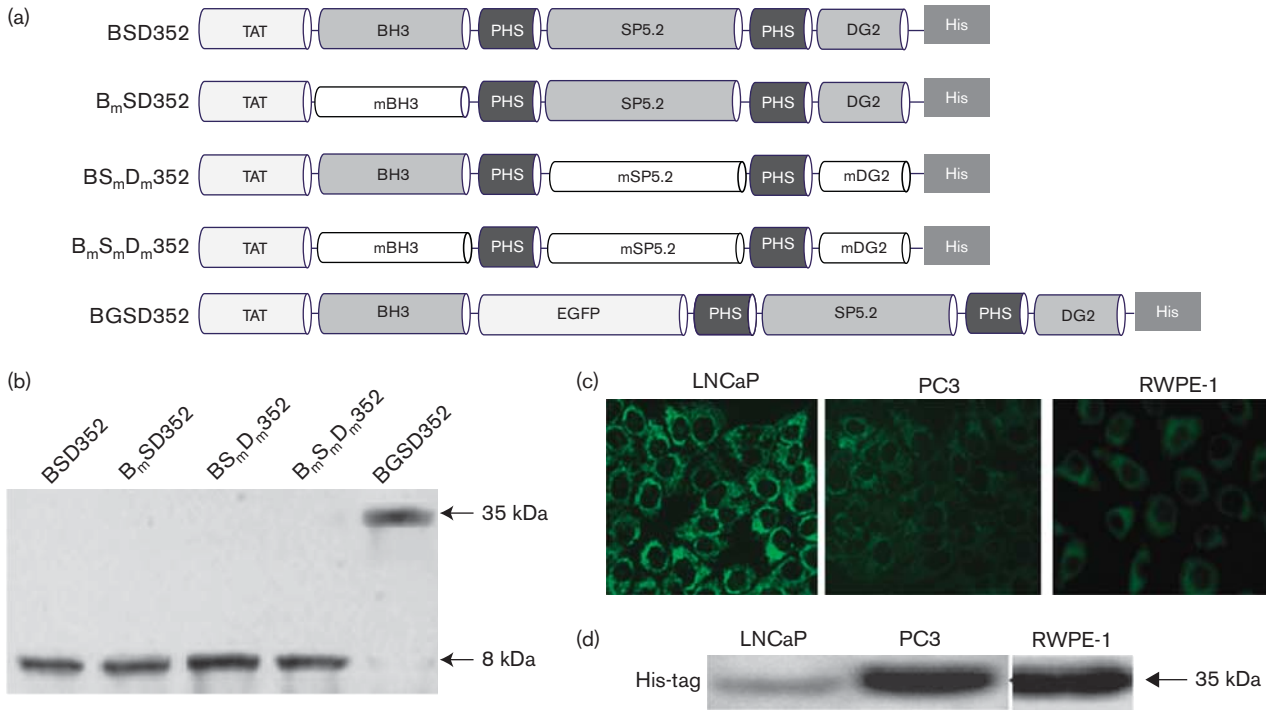

Design and expression of fusion proteins and their permeability. (a) Schematic diagram of the constructs of BSD352 and different mutated or control fusogenic peptides. (b) Western blot analysis of fusion protein expression: The details of the hybridization conditions are described above. (c) BGSD352 permeability analysis. Obvious green fluorescence was observed in LNCaP cells, but it was weak in both PC3 and RWPE-1 cells. (magnification: $\times$ 200). (d) BGSD352 cleavage analysis. Western blot results using the anti-His antibody showing a weak band in the LNCaP cells and a strong specific band in the PC3 and RWPE-1 cells, which indicated the cleaved and intact forms of BGSD352-His, respectively. EGFP, enhanced green fluorescent protein; PHS, PSA hydrolytic substrate; TAT, transactivating regulatory protein.

Table 1 The oligonucleotides for different fusion peptides

Domains	Amino acid	Deduced sequence
HIV TAT	YGRKKRRQRRR	5′-*catatg*TATGGCAGAAAAAAAAGAAGACAGAGAAGAAGA-3′
PUMA BH3	IGAQLRRMADDLNAQ	5′-ATTGGCGCGCAGTTAAGAAGAATGGCGGATGATTTAAACGCGCAG-3′
Mutated BH3	IGAQLRR*A*Y*D*LNAQ	5′-ATTGGCGCGCAGTTAAGAAGA*ATT*GCG*TAT*GATTTAAACGCGCAG-3′
VEGF-SP5.2	NGYEIEWYSWVTHGMY	5′-AACGGCTATGAAATTGAATGGTATAGCTGGGTGACCCATGGCATGTAT-3′……
Mutated SP5.2	NGYEIEW*S*SWVTHGMY	5′-AACGGCTATGAAATTGAATGG*AGC*AGCTGGGTGACCCATGGCATGTAT-3′
bFGF-DG2	KRTGQYKL	5′-AAAAGAACCGGCCAGTATAAATTA*gaattc*-3′
Mutated DG2	K*S*TG*T*YKL	5′-AAA*AGC*ACCGGC*ACC*TATAAATTA*gaattc*-3′
PSA hydrolytic substrate peptide	HSSKLQ	5′-CATAGCAGCAAATTACAG-3′

The oligonucleotides corresponding to different functional peptides and PHS peptide were back translated from amino acid sequences using codons optimized for *E. coli* expression. The mutated sites were underlined and marked in italic. The restriction enzyme sites that were incorporated to facilitate ligation were underlined with lowercase characters in italic.
bFGF, basic fibroblast growth factor; PSA, prostate-specific antigen; PUMA, p53 upregulated modulator of apoptosis; TAT, transactivating regulatory protein; VEGF, vascular endothelial growth factor.

570 nm using a microplate reader (Bio-Rad550). The protracted cell growth curve and the inhibitory rates of cell growth were calculated based on the absorbance value as follows: inhibitory rate = $(1–A_{\text{treated group}}/A_{\text{untreated group}}) \times 100\%$. All experiments were performed as three independent experiments.

In-vitro apoptosis analysis

LNCaP, PC3, and RWPE-1 cells were treated with the BS_mD_m352 and $B_mS_mD_m352$ fusion peptides at a concentration of 45 μmol/l for 24 h. For acridine orange/ethidium bromide (AO/EB) staining, the cells grown on coverslips were rinsed and treated with a solution composed of AO/EB (100 mg/l PBS of each dye) according to the manufacturer's instruction (Keygen Biotech. Co. Ltd., Nanjing, China). The cells were then examined under a fluorescence microscope. At least 300 cells were counted under the fluorescence microscope to quantify apoptosis. For flow cytometry analysis, 1×10^6 cells were harvested and washed in cold PBS, and then resuspended in binding buffer followed by labeling with fluorescein isothiocyanate-conjugated annexin V (annexin

V–fluorescein isothiocyanate; Santa Cruz Biotechnology, Santa Cruz, California, USA) for 20 min in the dark. The cells were then washed and analyzed by a FACS-Calibur Flow Cytometry system (BD Biosciences, Sparks, Maryland, USA) and the percentage of apoptotic cells was calculated using the WinMDI software (BD Biosciences). All experiments were performed as three independent experiments.

Western blot analysis

LNCaP and PC3 cells, treated with BS_mD_m352 and $B_mS_mD_m352$ at a concentration of 45 μmol/l for 24 h, were harvested and lysed in lysis buffer on ice. The cell extracts were clarified by centrifugation and the protein concentrations were determined using the Bio-Rad protein assay kit (Bio-Rad). The cell extract (25 μg of total protein) was then analyzed by SDS-PAGE and western blot. The primary antibodies used in this experiment were monoclonal antibodies of mouse anti-BAX, cytochrome C, His-tag, β-actin (Santa Cruz Biotechnology), and caspase 9 (Abcam, UK). The goat anti-mouse immunoglobulin G coupled with horseradish peroxidase (Santa Cruz Biotechnology) was used as the secondary antibody for the detection of protein expression.

In-vivo tumor growth inhibition assay

Athymic (*nu/nu*) nude mice (8 weeks old) were obtained from the Animal Center of the Fourth Military Medical University (Xi'an, China) and housed in laminar flow cabinets under specific pathogen-free conditions. All animal studies were carried out in compliance with the Medicine Institutional Guidelines of the Fourth Military Medical University. Aliquots of 1.0×10^6 LNCaP cells were suspended in 1 : 1 PBS mixed with matrigel (BD Biosciences) and subcutaneously inoculated into the right flank of each mouse. When 200–300 mm^3 tumors were observed, the mice were randomly assigned to five groups ($n = 5$) that received 60 μl of 120 μmol/l BSD352, BS_mD_m352, B_mSD352, $B_mS_mD_m352$, or PBS intratumorally, respectively, every 2 days for 14 days. After 14 days, the mice were killed to harvest tumors for further analysis. The tumors were then measured with a caliper and their volumes were calculated using the following standard formula: $\text{width}^2 \times \text{length} \times 0.5$.

Tumor tissue staining for in-vivo apoptosis and antiangiogenesis analysis

Frozen sections of the tumor tissues were used to conduct the terminal deoxynucleotidyl transferase dUTP nick end labeling assay according to the manufacturer's instructions (Nanjing Keygen Biotech. Co, Ltd.). The apoptotic cells were observed under a light microscope and at least 300 cells were counted. All experiments were performed as three independent experiments. For in-vivo antiangiogenesis analysis, the intratumoral microvessel density was analyzed on sections of paraffin-embedded LNCaP xenograft tumors using a mouse anti-human CD31 monoclonal antibody (Zhongshan Biotechnology, Beijing, China) and Vectastain ABC kit (Vector Laboratories, Burlingame, California, USA). Microvessel density was assessed initially by scanning the tumor at low power, followed by the identification of eight areas containing the maximum number of discrete microvessels and by counting the individual microvessels under low magnification (× 100).

Prostate-specific antigen measurement

A PSA detection kit from Roche Inc. (San Diego, California, USA) was used for measurement of PSA levels in both the cell culture media (secreted) and serum of the LNCaP xenografts mouse. In brief, LNCaP and PC3 prostate cancer cells were maintained in phenol red-free RPMI 1640 medium, whereas RWPE-1 cells were cultured in keratinocyte serum-free medium for 72 h. Next, the culture media were collected and the detached cells were removed by centrifugation, respectively. For LNCap xenografts mice, serum was collected by retro-orbital bleeding before drug administration, when 200–300 mm^3 tumors were observed. Both the cell culture media and serum PSA level were measured by the Roche E 170 module for MODULAR ANALYTICS EVO analyser (Roche Inc.).

Statistical analysis

All statistical analyses were carried out by using SPSS 13.0 (IBM Company, Chicago, USA). Data are expressed as mean ± standard deviation. Comparisons among all the groups were made using the one-way analysis of variance test and the Student–Newman–Keuls method. Differences were considered statistically significant at P less than 0.05.

Results

Design of expression vectors and expression and purification of fusion proteins

To evaluate the potency of PSA-activated fusion peptide BSD352 as a dual-targeted therapy strategy for prostate cancer, we generated expression vectors for BSD352, B_mSD352, BS_mD_m352, $B_mS_mD_m352$, and BGSD352 (Fig. 1a) and expressed the fusion proteins in bacterial cells. Western blot analysis of the expressed products with the anti-His antibody showed that the recombinant proteins showed expected molecular weights at approximately 8 kDa and 35 kDa (Fig. 1b). All fusion proteins were expressed at high levels (approximately 55 mg/l culture) and could be highly enriched using the His-tag protein purification system under native conditions.

PSA cleavage and BH3 peptide permeable analysis

We first used BGSD352 to determine whether the fusion proteins with TAT PTD can translocate into the tumor cells. As shown in Fig. 1c, green fluorescence was readily observed under a fluorescence microscope in both the PSA-producing LNCaP cells and non-PSA producing

PC3 and RWPE-1 cells after treatment with 45 μmol/l BGSD352 for 4 h, indicating that BGSD352 proteins, both in the cleaved and intact form, were able to transduce into PSA-producing and nonproducing tumor cells. Then, we examined the presence of His-tag within the BGSD352-treated LNCaP, PC3, and RWPE-1 cells by Western blot analysis. As shown in Fig. 1d, no His-tag protein was detected in the BGSD352-treated LNCaP cells whereas a clear band at position 35 kDa, corresponding to the full-length form of BGSD352, was readily detected in the BGSD352-treated PC3 and RWPE-1 cells, which indicates that the purified BGSD352 fusion proteins could be transduced into the tumor cells and also efficiently cleaved by PSA in the PSA-producing cells.

In-vitro cell proliferation and apoptosis analysis

BH3 has been known to disrupt mitochondrial membranes and induce cell apoptosis. Here we tested cell viability after BS_mD_m352 treatment using the MTT assay. As shown in Fig. 2, 5 μmol/l of BS_mD_m352 could inhibit proliferation of LNCaP cells, and the inhibition rates were found to increase with increased concentrations of BS_mD_m352. In contrast, no notable growth-inhibitory effect was observed in the $B_mS_mD_m352$-treated LNCaP, PC3, and RWPE-1 cells or the BS_mD_m352-treated PC3 and RWPE-1 cells ($P < 0.01$, versus LNCaP/BS_mD_m352). We further investigated whether BS_mD_m352 treatment could induce tumor cell apoptosis by AO/EB staining and flow cytometry analysis. As shown in Fig. 3a and b, BS_mD_m352 treatment at 45 μmol/l for 24 h efficiently induced high-level apoptosis of LNCaP cells. In comparison, only low-level cell apoptosis was observed in the BS_mD_m352-treated PC3 and RWPE-1 cells and the $B_mS_mD_m352$treated LNCaP, PC3, and RWPE-1 cells.

BH3 peptide activates mitochondrial pathway apoptosis

The cell apoptosis may proceed in two major pathways: an intrinsic and an extrinsic apoptotic signaling pathway [25,26]. It has been reported earlier that BH3 peptide treatment potently results in the disruption of heterodimerization interactions between the proapoptotic and antiapoptotic Bcl-2 family members and activates the intrinsic apoptosis pathway. To further investigate the underlying mechanism for BS_mD_m352-induced LNCaP cells apoptosis, we conducted a western blot analysis to analyze the expression of cellular proteins that are associated with the mitochondria-related apoptotic pathway. The results showed elevated expression of Bax, cytochrome C, and caspase-9 cleavage (Fig. 3c) only in the BS_mD_m352-treated LNCaP cells, which further confirmed that the BS_mD_m352 fusion peptide, after digestion by PSA, released the functionally active TAT-BH3 peptide and induced the intrinsic pathway of tumor cell apoptosis.

BSD352 induces xenograft tumor cell apoptosis and inhibits tumor growth

To determine the in-vivo tumor growth-inhibitory effect, BSD352, BS_mD_m352, B_mSD352, and $B_mS_mD_m352$ were injected intratumorally every 2 days for 14 days. Compared with the $B_mS_mD_m352$-treated or PBS-treated tumor, administration of BSD352, BS_mD_m352, and B_mSD352 led to significant tumor growth inhibition, although at different levels with an inhibition rate of 81.69 ± 6.91, 47.11 ± 4.61, and $36.06 \pm 3.55\%$, respectively, indicating that the presence of all three functional domains in the BSD352 fusion protein synergized the inhibition effect ($P < 0.01$ and < 0.05, respectively) (Fig. 4a). We further carried out terminal deoxynucleotidyl transferase dUTP nick end labeling staining on tumor sections from mice treated with different fusion proteins, and the results showed that treatment with BSD352 and BS_mD_m352 induced tumor cells apoptosis throughout 60% of the total tumor cells, whereas the B_mSD352-and $B_mS_mD_m352$-treated tumor cells did not show any obvious apoptotic cells (Fig. 4b).

BSD352 inhibits endothelial cell growth *in vitro*

To confirm that the SP5.2 and DG2 peptides reported earlier could still play a role in the in-vitro antiangiogenesis of the BSD352 construct, we conducted the MTT assay using HUVE cells. The results showed that PSA-predigested B_mSD352 significantly inhibited the growth of HUVE cells compared with the $B_mS_mD_m352$-treated HUVE cells (Fig. 5a), which showed that BSD352, after hydrolysis by PSA in prostate cancer cells, could release the active form of antiangiogenic SP5.2 and DG2 peptides *in situ* and inhibit HUVE cells proliferation *in vitro*.

BSD352 inhibits angiogenesis *in vivo*

To investigate whether the reduced size of the BSD352-treated LNCaP xenograft tumors was correlated in part with reduced neovascularization *in vivo*, we conducted immunohistochemistry staining with an anti-human CD31 antibody in the BSD352-treated, B_mSD352-treated, and $B_mS_mD_m352$-treated LNCaP xenograft tumor sections to quantify the density of microvessels. The results showed that tumors treated with BSD352 and B_mSD352 led to a significant reduction of CD31-positive blood vessels compared with the $B_mS_mD_m352$-treated or PBS-treated tumors (Fig. 5b), which further confirmed the in-vivo angiogenic effects of SP5.2 and DG2 peptides.

PSA level in different cells and xenograft mouse serum

Measurement of the PSA level showed that LNCaP prostate cancer cells not only secreted high levels of PSA in the cultured media (61 ng/ml, average of three samples), but also produced high levels of PSA in the serum of a xenograft mouse (20 ng/ml, average of three mice) when the tumor grew to a size of approximately

Fig. 2

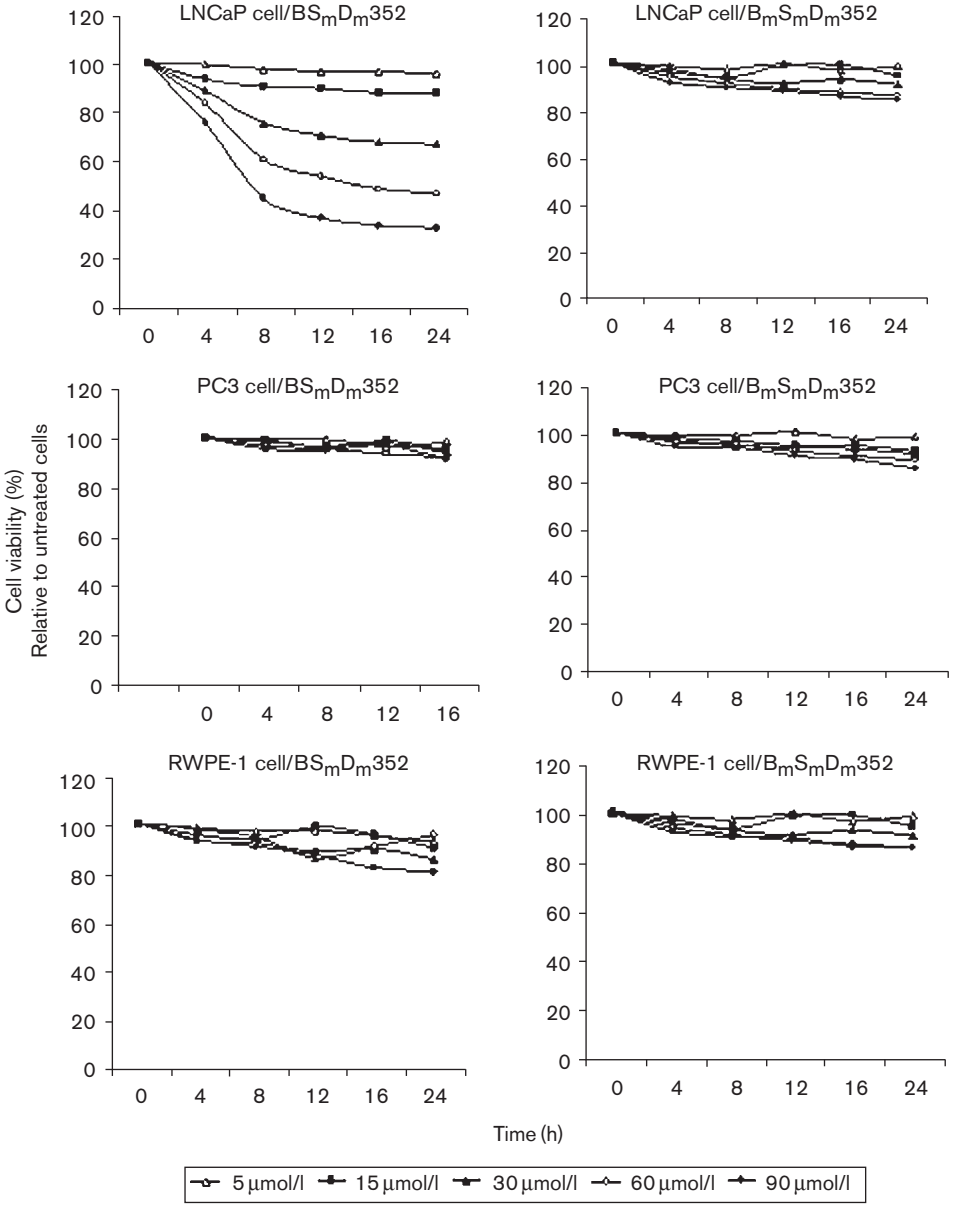

Proliferation analysis of LNCaP, PC3, and RWPE-1 cells treated with BS_mD_m352. MTT assay results showed that LNCaP cells treated with BS_mD_m352 showed increased proliferation inhibition with increased BS_mD_m352 concentration and treating time, unlike PC3 and RWPE-1 cells. ($P<0.05$ vs. LNCaP/BS_mD_m352).

200 mm^3. However, there was only basal level of PSA secreted in both the PC3 and RWPE-1 cells' culture media (0.06 ng/ml and 0.4 ng/ml, respectively).

Discussion

The development of targeted prodrugs for delivering sufficient amounts of tumor-targeted drugs while minimizing the damage to the surrounding normal tissues is an important goal in anticancer research currently. One method of targeting antitumor drugs to prostate cancer is to use PSA [27,28].

In this study, we designed a multifunctional fusion peptide, BSD352, and investigated its potential application as a prodrug for prostate cancer therapy. Whether BH3, SP5.2, and DG2 peptides in BSD352 could separately perform their function was mainly determined by efficient PSA cleavage and TAT-BH3 cells permeability for their correct localization. The HIV-1-derived TAT PTD peptide renders various macromolecules cell permeable [21,29]. By using the PSA-producing LNCaP cells, non-PSA producing PC3 cells, and normal human

Fig. 3

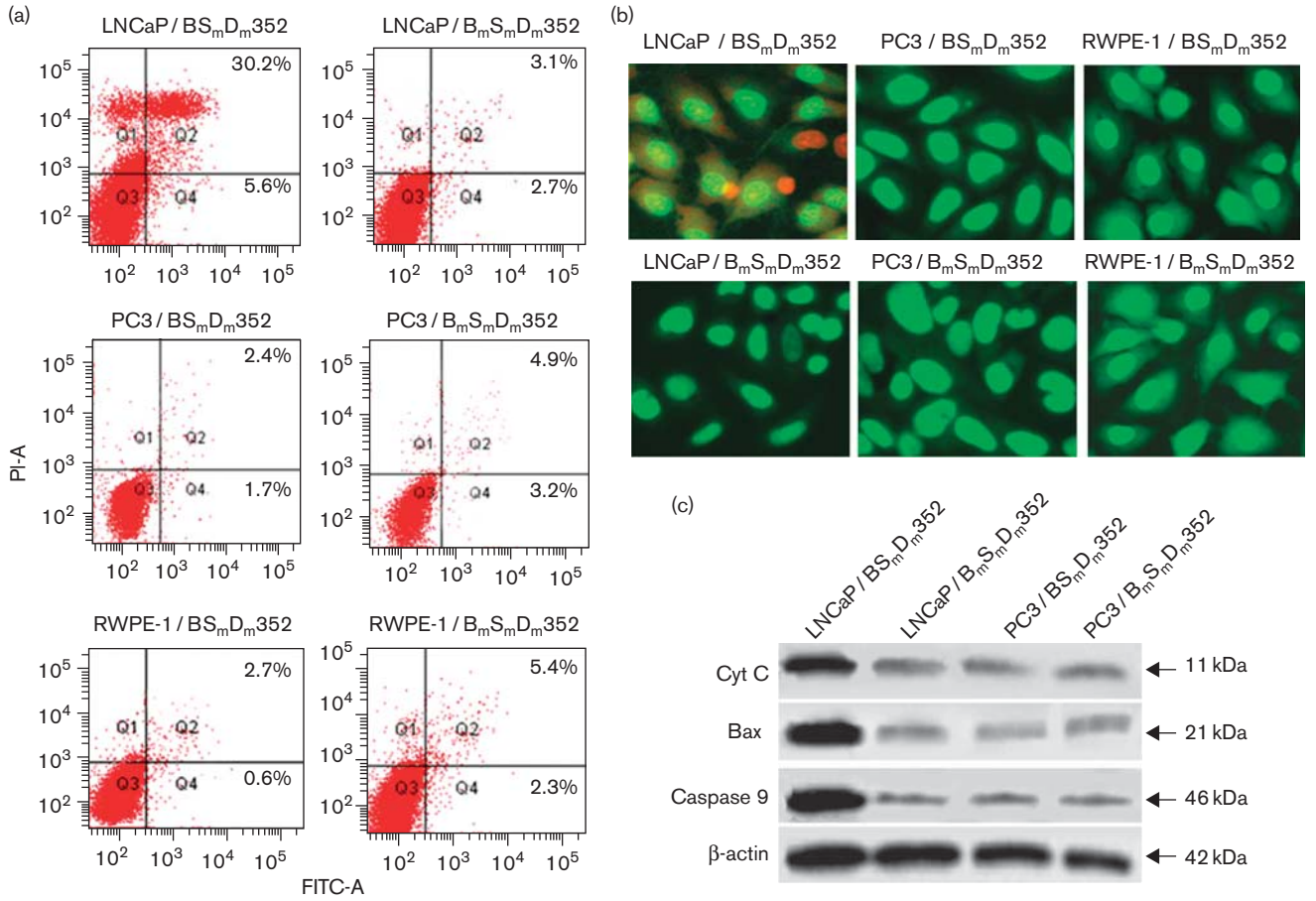

Apoptosis analysis of LNCaP, PC3, and RWPE-1 cells treated with BS_mD_m352. (a) Flow cytometry results showing that BS_mD_m352 treatment induced nearly 50% of LNCaP cells apoptosis, whereas no obvious apoptotic signals were observed in the other two cells. (b) Acridine orange/ethidium bromide double staining showing green with bright green dots or orange staining in the nuclei of BS_mD_m352-treated LNCaP cells (positive) and uniformly green staining in the nuclei of $B_mS_mD_m352$-treated LNCaP and the other two cells treated with both BS_mD_m352 and $B_mS_mD_m352$ (negative) (magnification: × 200). (c) Western blot analysis confirming the mitochondrial pathway of apoptosis. BS_mD_m352-treated LNCaP cells showed elevated expression of all three intrinsic apoptosis markers. FITC, fluorescein isothiocyanate; PI, propidium iodide.

prostatic epithelial cell RWPE-1, we analyzed BSD352 cleavage by PSA and its translocation property to enter the cells. As a His-tag segment was fused to the C-terminus of all fusion peptides and the cleavage of the fusion peptide by PSA was done outside the cancer cells, the western blot detection of His-tag within the BGSD352-treated cells was evidence of the intact form, whereas the His-tag detection negative with fluorescence observation positive represented the cleaved form of the fusion peptide. The results from Fig. 1c and d showed that the BGSD352 peptide had been efficiently cleaved into three different peptides by PSA, as designed by us, in the extracellular fluid surrounding the prostate cancer cells and that the TAT-BH3 peptide rapidly transduced nearly 100% of the LNCaP cells *in vitro*. The ability of BSD352 to be cleaved and efficiently transferred into the LNCaP cancer cells set the foundation to further test its activity in an animal model for the treatment of prostate cancers.

Earlier studies have shown that the BH3 peptide derived from proapoptotic proteins can disrupt the heterodimerization of Bcl-x_l and Bcl-2 with proapoptotic binding partners in a highly specific manner, and induce apoptosis through the mitochondrial pathway in a broad range of cancer cells [30–34]. We observed that BS_mD_m352 treatment not only inhibited proliferation of LNCaP cells and induced tumor cells apoptosis, but also resulted in elevated levels of Bax, cytochrome C release, and cleavage of caspase-9. These results indicate that the BH3 domain of BSD352 may directly trigger the intrinsic pathway to induce apoptosis in prostate cancer cells. This in-vitro apoptosis-inducing effect was further confirmed by in-vivo injection of BS_mD_m352, which inhibited xenograft tumor growth (Fig. 4a). Although BH3 peptide has a powerful apoptosis-inducing activity, its antitumor effect is still limited when used *in vivo*. Therefore, the SP5.2 and DG2 peptides, which were shown to have a

Fig. 4

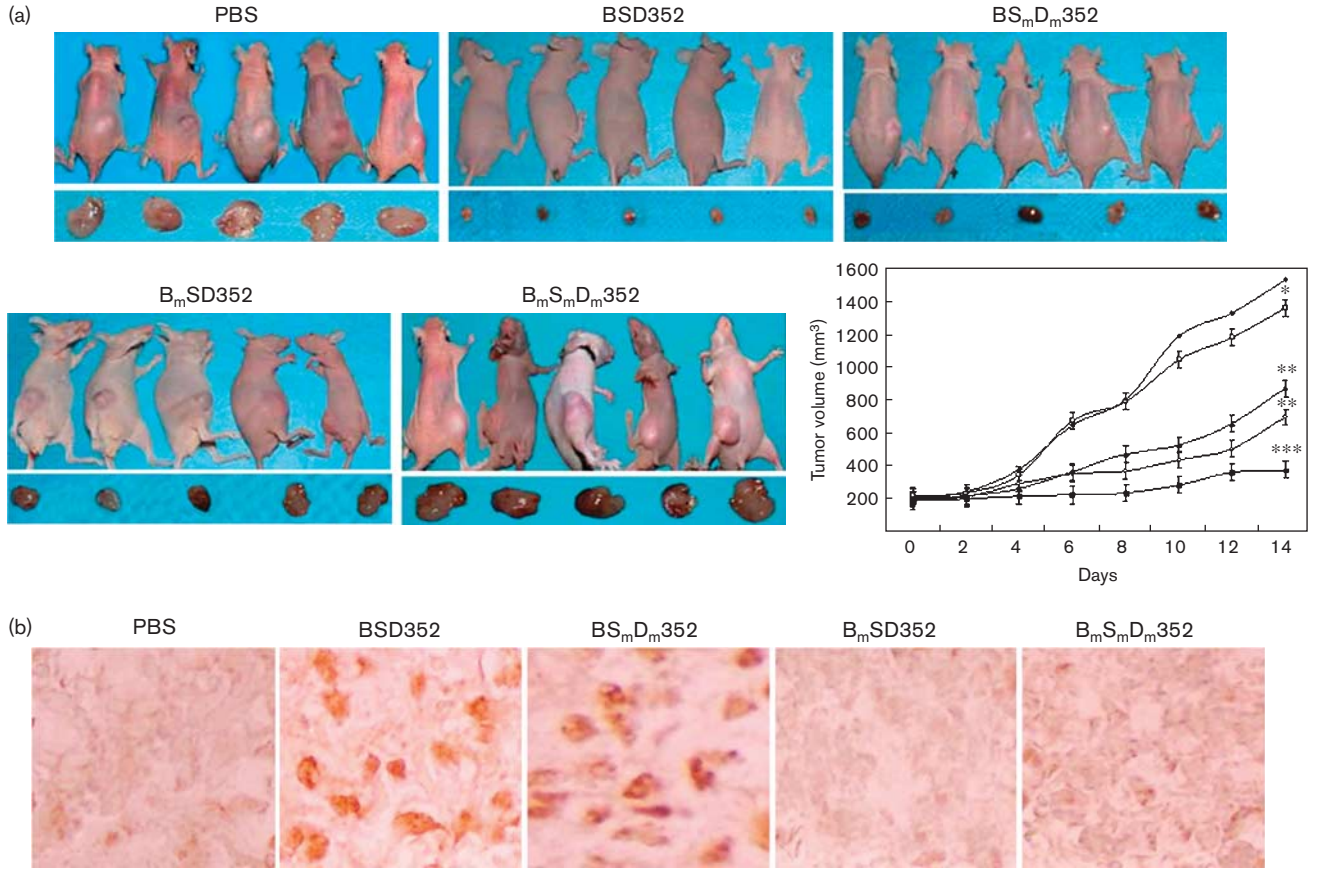

In-vivo apoptosis induction and tumor growth inhibition. (a) LNCaP xenograft tumor size 14 days after administration of different fusion proteins $*P>0.05$; $**P<0.05$; $***P<0.01$; versus PBS-treated control. (b) Terminal deoxynucleotidyl transferase dUTP nick end labeling staining of xenograft tumor tissues showing strong, positive dark brown signals in the nucleus of the BSD352-treated and BS_mD_m352-treated tumor cells compared with the control cells (magnification: $\times 200$).

strong angiogenic inhibitory effect, both *in vitro* and *in vivo* [22,23], were incorporated into the BSD352 construct by PHS peptides to augment the antitumor effect of the BH3 peptide.

In addition to inducing tumor cell apoptosis, tumor angiogenesis is also considered as a useful target for anticancer therapy [35,36], as solid tumor growth and metastasis are dependent on tumor vascularization. Our in-vitro proliferation results showed that B_mSD352 significantly inhibited growth of HUVE cells, which agrees with the reported function of SP5.2 and DG2 [22,23]. We further observed that tumors treated with B_mSD352 containing a mutated BH3 peptide and wild-type SP5.2 and DG2 peptides, targeting VEGF and bFGF have a marked decrease in tumor vessel density and tumor growth inhibition rate compared with the $B_mS_mD_m352$-treated or PBS-treated tumor. More significantly, the BSD352-treated xenograft tumors showed more profound tumor growth inhibition compared with the BS_mD_m352-, B_mSD325-, and $B_mS_mD_m352$-treated tumors, which showed the synergistic enhancement of tumor inhibition by the combination of proapoptotic peptides and anti-angiogenic peptides.

Despite the encouraging inhibitory effect of BSD352 on the growth of PSA-secreting prostate cancer, further analysis on the systematic delivery of this construct to prostate tumor is still required. As serum PSA is at a 1000-fold to 10 000-fold lower concentration in the circulating fluid and is catalytically inactive because it circulates bound to α_1-antichymotrypsin and α_2-macroglobulin, the therapeutic efficacy of BSD352 should be achieved [16]. Moreover, as BSD352 inhibits prostate tumor growth by inducing cancer cells apoptosis through the BH3-triggered mitochondrial pathway and by inhibiting angiogenesis, it can be used for PSA-secreting androgen-reliant prostate cancer therapy, and this strategy also provides a methodology for the treatment of androgen-refractory prostate cancer, which does not produce PSA, by replacement of the hydrolytic substrate peptide with a different protease peptide secreted by prostate cancer cell such as human glandular kallikrein 2 [37].

Fig. 5

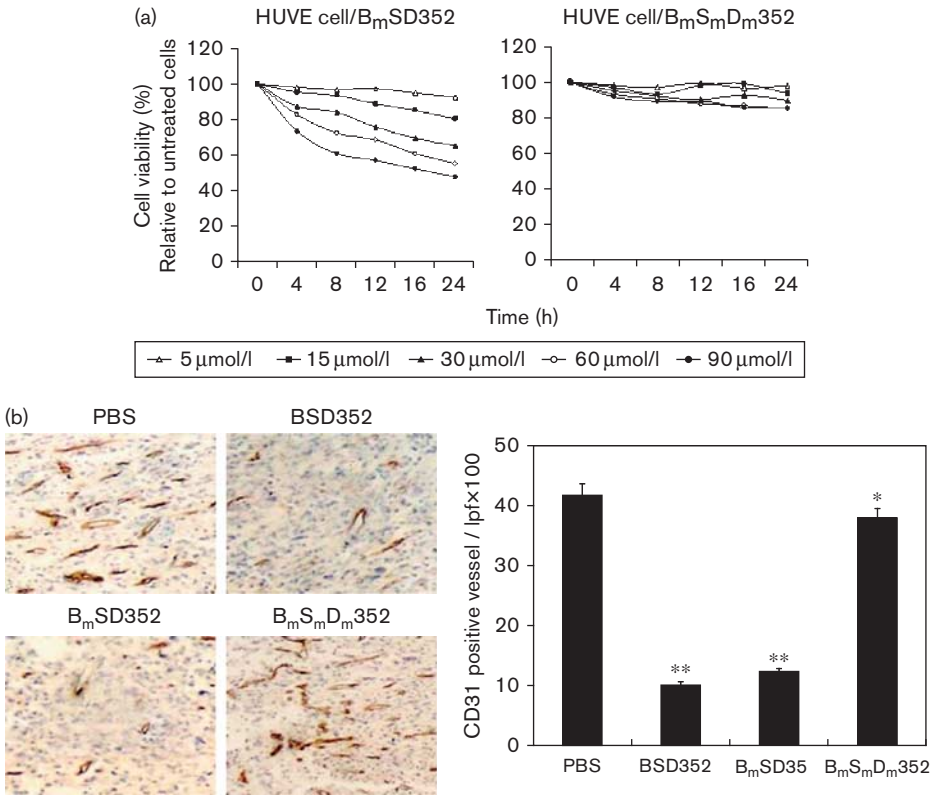

Antiangiogenic analysis of BSD352 *in vitro* and *in vivo*. (a) B_mSD352 inhibited HUVE cells growth in a dose-dependent and time-dependent manner. (b) Blood vessel quantification in xenograft tumors with anti-CD31 antibody staining. LPF, low-power field ($\times$ 100). *$P>0.05$; **$P<0.05$, versus PBS-treated control.

Taken together, our data provide proof-of-concept that the fusion protein BSD352 induces apoptosis in the PSA-producing prostate cancer cells and inhibits vascular endothelium proliferation in both in-vitro and in-vivo studies. This tumor site-specific target therapy may overcome the adverse effects caused by the current use of systemic therapy drugs, and may increase the therapeutic index with the potential to reduce tumor burden alone or when coadministered with conventional chemotherapy.

Acknowledgements

The authors thank everyone of the department of Laboratory Medicine for their technical support. This study was supported by a Grant from the National Natural Science Foundation of China (30600617).

References

1 Shao YH, Demissie K, Shih W, Mehta AR, Stein MN, Roberts CB, *et al.* Contemporary risk profile of prostate cancer in the United States. *J Natl Cancer Inst* 2009; **101**:1280–1283.
2 Cookson MM. Prostate cancer: screening and early detection. *Cancer Control* 2001; **8**:133–140.
3 Denmeade SR, Isaacs JT. A history of prostate cancer treatment. *Nat Rev Cancer* 2002; **2**:389–396.
4 Dorff TB, Quek ML, Daneshmand S, Pinski J. Evolving treatment paradigms for locally advanced and metastatic prostate cancer. *Expert Rev Anticancer Ther* 2006; **6**:1639–1651.
5 Swanson G, Thompson I, Basler J, Crawford ED. Metastatic prostate cancer-does treatment of the primary tumor matter? *J Urol* 2006; **176**:1292–1298.
6 Balk SP. Androgen receptor as a target in androgen-independent prostate cancer. *Urology* 2002; **60**:132–139.
7 Klotz L. Hormone therapy for patients with prostate carcinoma. *Cancer* 2000; **88**:3009–3014.
8 Culig Z, Bartsch G. Androgen axis in prostate cancer. *J Cell Biochem* 2006; **99**:373–381.
9 Agus DB, Cordon-Cardo C, Fox W, Drobnjak M, Koff A, Golde DW, *et al.* Prostate cancer cell cycle regulators: response to androgen withdrawal and development of androgen independence. *J Natl Cancer Inst* 1999; **91**:1869–1876.
10 Denmeade SR, Lin XS, Isaacs JT. Role of programmed (apoptotic) cell death during the progression and therapy for prostate cancer. *Prostate* 1996; **28**:251–265.
11 Knudsen KE, Arden KC, Cavenee WK. Multiple G1 regulatory elements control the androgen-dependent proliferation of prostatic carcinoma cells. *J Biol Chem* 1998; **273**:20213–20222.
12 Loblaw DA, Virgo KS, Nam R, Somerfield MR, Ben-Josef E, Mendelson DS, *et al.* Initial hormonal management of androgen-sensitive metastatic, recurrent, or progressive prostate cancer. *J Clin Oncol* 2007; **25**: 1596–1605.
13 Sowery RD, So AI, Gleave ME. Therapeutic options in advanced prostate cancer: present and future. *Curr Urol Rep* 2007; **8**:53–59.
14 Basler M, Groettrup M. Advances in prostate cancer immunotherapies. *Drugs Aging* 2007; **24**:197–221.
15 Gupta S. Prostate cancer chemoprevention: current status and future prospects. *Toxicol Appl Pharmacol* 2007; **224**:369–376.
16 LeBeau AM, Singh P, Isaacs JT, Denmeade SR. Potent and selective peptidyl boronic acid inhibitors of the serine protease prostate-specific antigen. *Chem Biol* 2008; **15**:665–674.

17 Appelmann I, Liersch R, Kessler T, Mesters RM, Berdel WE. Angiogenesis inhibition in cancer therapy: platelet-derived growth factor (PDGF) and vascular endothelial growth factor (VEGF) and their receptors: biological functions and role in malignancy. *Recent Results Cancer Res* 2010; **180**:51–81. (Review).

18 D'Andrea LD, Del Gatto A, De Rosa L, Romanelli A, Pedone C. Peptides targeting angiogenesis related growth factor receptors. *Curr Pharm Des* 2009; **15**:2414–2429. (Review).

19 Pötgens AJ, Westphal HR, De Waal RM, Ruiter DJ. The role of vascular permeability factor and basic fibroblast growth factor in tumor angiogenesis. *Biol Chem Hoppe Seyler* 1995; **376**:57–70.

20 Ho A, Schwarze SR, Mermelstein SJ, Waksman G, Dowdy SF. Synthetic protein transduction domains: enhanced transduction potential *in vitro* and *in vivo*. *Cancer Res* 2001; **61**:474–477.

21 Schwarze SR, Dowdy SF. *In vivo* protein transduction: intracellular delivery of biologically active proteins, compounds and DNA. *Trends Pharmacol Sci* 2000; **21**:45–48.

22 El-Mousawi M, Tchistiakova L, Yurchenko L, Pietrzynski G, Moreno M, Stanimirovic D, *et al.* A vascular endothelial growth factor high affinity receptor 1-specific peptide with antiangiogenic activity identified using a phage display peptide library. *J Biol Chem* 2003; **278**:46681–46691.

23 Yayon A, Aviezer D, Safran M, Gross JL, Heldman Y, Cabilly S, *et al.* Isolation of peptides that inhibit binding of basic fibroblast growth factor to its receptor from a random phage2 epitope library. *Proc Natl Acad Sci U S A* 1993; **90**:10643–10667.

24 Gao P, Wang R, Shen J-J, Lin F, Wang X, Dong K, *et al.* Hypoxia-inducible enhancer/a-fetoprotein promoter-driven RNA interference targeting STK15 suppresses proliferation and induces apoptosis in human hepatocellular carcinoma cells. *Cancer Sci* 2008; **99**:2209–2217.

25 Weinmann M, Jendrossek V, Handrick R, Güner D, Goecke B, Belka C. Molecular ordering of hypoxia-induced apoptosis: critical involvement of the mitochondrial death pathway in a FADD/caspase-8 independent manner. *Oncogene* 2004; **23**:3757–3769.

26 Weinmann M, Jendrossek V, Handrick R, Güner D, Goecke B, Belka C. FOXO3a-dependent regulation of Puma in response to cytokine/growth factor withdrawal. *J Exp Med* 2006; **203**: 1657–1663.

27 Madan RA, Arlen PM, Mohebtash M, Hodge JW, Gulley JL. Prostvac-VF: a vector-based vaccine targeting PSA in prostate cancer. *Expert Opin Investig Drugs* 2009; **18**:1001–1011.

28 Isaacs JT. New strategies for the medical treatment of prostate cancer. *BJU Int* 2005; **96**:35–40.

29 Harada H, Kizaka-Kondoh S, Hiraoka M. Antitumor protein therapy; application of the protein transduction domain to the development of a protein drug for cancer treatment. *Breast Cancer* 2006; **13**:16–26.

30 Finnegan NM, Curtin JF, Prevost G, Morgan B, Cotter TG. Induction of apoptosis in prostate carcinoma cells by BH3 peptides which inhibit Bak/Bcl-2 interactions. *Br J Cancer* 2001; **85**:115–121.

31 Shangary S, Johnson DE. Peptides derived from BH3 domains of Bcl-2 family members: a comparative analysis of inhibition of Bcl-2, Bcl-x(l) and Bax oligomerization, induction of cytochrome C release, and activation of cell death. *Biochemistry* 2002; **41**:9485–9495.

32 Shangary S, Oliver CL, Tillman TS, Cascio M, Johnson DE. Sequence and helicity requirements for the proapoptotic activity of Bax BH3 peptides. *Mol Cancer Ther* 2004; **3**:1343–1354.

33 Lomonosova E, Chinnadurai G. BH3-only proteins in apoptosis and beyond: an overview. *Oncogene* 2008; **27**:2–19.

34 Willis SN, Fletcher JI, Kaufmann T, Van Delft MF, Chen L, Czabotar PE, *et al.* Apoptosis initiated when BH3 ligands engage multiple Bcl-2 homologs, not Bax or Bak. *Science* 2007; **315**:856–859.

35 Thoenes L, Günther M. Novel approaches in anti-angiogenic treatment targeting endothelial F-actin: a new anti-angiogenic strategy? *Curr Opin Mol Ther* 2008; **10**:579–590.

36 Norden AD, Drappatz J, Wen PY. Novel anti-angiogenic therapies for malignant gliomas. *Lancet Neurol* 2008; **7**:1152–1160.

37 Janssen S, Jakobsen CM, Rosen DM, Ricklis RM, Reineke U, Christensen SB, *et al.* Screening a combinatorial peptide library to develop a human glandular kallikrein 2-activated prodrug as targeted therapy for prostate cancer. *Mol Cancer Ther* 2004; **11**:1439–1450.